# Nucleation and Growth During the Crystallization of Amorphous Tellurium Thin Films

Primary Investigator: Vin Anand

MSE 130: Experimental Materials Science and Design

University of California, Berkeley

*September 28, 2020*

**Table of Contents:**

**Abstract:**

Nucleation is a thermally activated process which can be used to develop high quality crystalline semiconductor materials on any non-crystalline substrate at low temperatures. This study explores the kinetics and crystallization of amorphous Tellurium with investigations into the low temperature growth of high-quality thin films on amorphous silica substrates. Classifying the fraction of a substrate area transformed over time at various different temperatures provides estimates of the energy barrier associated with the breaking of the amorphous bonds, and the formation of the crystalline bonds $\Delta E_{attachment}$, the free energy difference at peak cluster size $\Delta G(i_c)$, and the free energy reduction, represented by $g_{c\rightarrow a}$. These estimates were obtained by approximating the Arrhenius form curves for the nucleation rate per area, *N*, and the growth velocity of the grain, *v*. Taking into account the uncertainty and confidence level of the estimates, these measurements provide insights into the kinetics of Tellurium thin film nucleation on amorphous silica substrates. Pairing these values with information on the weighted mean surface energy of crystalline Tellurium gives an estimate on $i_c$ the number of atoms in a critical size cluster governing the growth kinetics, which was calculated to be approximately 1.29 atoms. Future studies on nucleation kinetics and crystallization of Tellurium thin films will allow for further innovation and applications in sensor and flexible display technologies, among other use cases.

## Introduction

Semiconductors offer a wide range of utility and applications in the technology and research sector. With the emergence of new hardware technologies such as wearable sensors and flexible displays, there is a need to develop high quality crystalline semiconductor materials on non-crystalline substrates at low temperatures. While the most prevalent semiconductor currently used is Silicon, Tellurium (*Te)* is another semiconductor that shows greater electrical conductivity with potential to be incorporated in future technology development. A bandgap of 0.32 eV and a low melting point $T_m$ of 449.5 degrees Celsius makes *Te* attractive for device fabrication, as thermal budgets can be kept very low allowing fabrication on a wide array of materials. As such, experiments were conducted to enable the direct measurement of the fraction of an amorphous *Te* thin film crystallized as a function of time for varying temperatures.

First order transitions including *Te* thin film creation, occur with nucleation and growth mechanism as described in classical nucleation theory [2]. In the amorphous to crystalline transformation of *Te*, there is a thermodynamic driving force for the formation of a solid phase for temperatures below the melting point $T_m$. As the temperature is lowered further, the liquid and amorphous phase free energies separate and the free energy reduction of these two states is represented by $g_{c\rightarrow a}$. *Figure 1* below depicts the temperature dependence of the free energies and the crystalline phase is still the most stable phase with the transformation from the amorphous phase to the crystalline phase reducing the free energy by the amount indicated as $g_{c\rightarrow a}$.

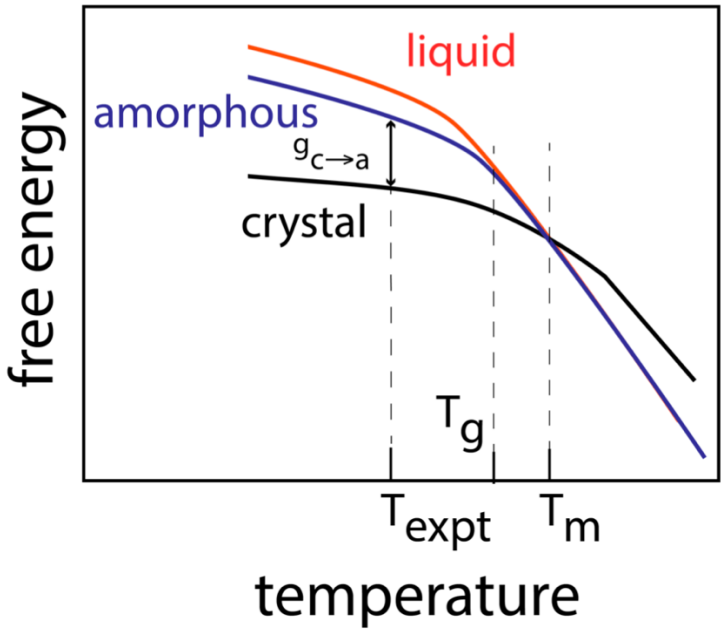


***Figure 1***. A schematic of the temperature dependence of the free energies of the three phases that could play a role in the experiment: the crystalline phase, the liquid phase, and the amorphous phase.

Within this transformation, the system reconfigures to minimize its Gibbs free energy, hence the transformation from amorphous to crystalline phase occurs. Our study aims to understand the governing kinetics behind this nucleation process and derive approximations for the free energy change during the amorphous to crystalline transformation and calculating the critical nucleus size. This information will allow researchers to optimize development of *Te* thin films and control the microstructure for various engineering applications.

**Experimental Procedure**

In order to obtain data for our analysis, experiments conducted by the Javey Research Group produced high quality *Te*-based field effect transistors (FETs) using a very low temperature deposition process, followed by annealing at 5 degrees Celsius [1]. First, Te is thermally deposited on a cold substrate held at -80◦ C using the Edwards 306 3 Thermal Evaporator with Te pellets (99.999%, Sigma-Aldrich) used as the thermal evaporation source. The deposition rate is approximately 10 Å $sec^{-1}$, and the thickness of the film is controlled using a quartz crystal microbalance. Typical film thicknesses were of the order of 4-20 nm. At the deposition temperature, the film is amorphous, as verified by x-ray diffraction experiments. After deposition, the sample temperature is increased rapidly to the desired temperature and then held at that temperature while the film continues to crystallize. The crystallization process is observed and recorded via optical microscopy. At very low temperatures, light stimulates crystallization, so the measurements at 5◦ Celsius had to be conducted very carefully by turning on the light only intermittently to get an image of the sample. To avoid this issue, we only consider crystallization at 10◦ Celsius and above. The *Te* sample is then warmed to room temperature and characterized.

Upon obtaining the images and optical frames for each trial in the temperature range from 10, 15, 20, 25, 30 and 35 degrees Celsius, we use computational techniques via iPython notebooks to classify the percent area transformed as a function of time for each experiment. Since the number of frames per experiment is in the thousands, we approximate our transformation rate using a subset of the images in our classification system. For the experiment data at 10 and 15 degrees Celsius, we use data collected at intervals of every 100 frames. For experiments at 20 and 25 degrees Celsius, we use data collected at intervals of every 50 frames. For experiments at 30 and 35 degrees Celsius, we use data collected at intervals of every 20 frames, as the total size of the

data lies under 1000 images. The frames were the loaded into a Python library known as *open cv2* which converts images to grayscale, then binarizes the pixels to either black or white clusters. With this image data as an array, we calculate the fraction of area transformed by summing the white clusters over total frame area since the RGB values for black and white pixels are respectively, 0 and 255. *Item A* of the Appendix discusses the image classification algorithm and computational techniques in further detail. Figure 2 below demonstrate how the program classifies and calculates the area fraction transformed at each timeframe.

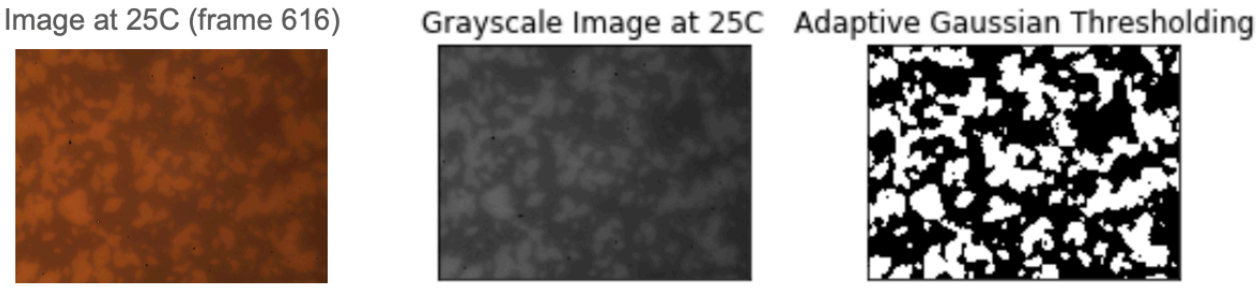


***Figure 2.*** Image classification using python open cv2 library. A frame from the 25 degrees Celsius trial is grayscale converted, then binarized to estimate and extract the fraction area transformed.

Adaptive gaussian thresholding is a technique which ensures that the binarization of each pixel occurs with a relative threshold in each region of the frame. Since the input data had lighting inconsistencies, we use this thresholding technique to increase the accuracy of our algorithm. Within each temperature category, we obtain between 80 to 120 data points of the fraction area nucleated of the substrate and the time. The next step is to use a plotting software and graph our data from each of the six experiments conducted. This analysis was conducted using Jupyter Notebook [4] and *Item C* in the appendix explains the plotting program and code in more depth. The plots for area fraction transformed versus time follow an approximate sigmoid shape, and seeing

as the values plotted fit the form of the Arrhenius equation, $\alpha = 1 - exp[-(\pi/3) * Nv^2 t]$, where $N$ is the nucleation rate per area $v$ is the growth velocity of the grain. Overlaying the sigmoid fitted curve allows us to extract the $Nv^2$ values for each experiment.

The next step in our process is to understand the density of grain growth for each temperature. Since we are not given any micrographs of the frames, we must assess the number of grains by manually counting the number of grains in a given region and multiply that ratio by the area of the frame. We are assuming consistent grain density throughout the frame. Similar to the area fraction transformed analysis, our process for density derivation uses a hybrid model where we manually count grains in a region and find the area density using *open cv2* as shown in Figure 3 below. Since we are given data in 70 $\mu$m and 140 $\mu$m we have to multiply fraction by the overall area consistent to the initial frame.

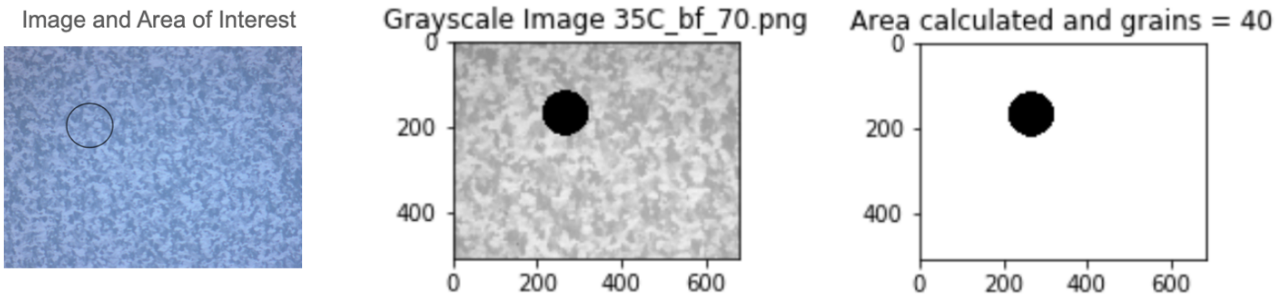


***Figure 3.*** Taking the frame at 35 degrees Celsius and 70 $\mu$m, we manually count the grains in the circular region then find the area fraction and extrapolate the density for the entire frame.

Applying the above analysis to all six temperature experiments, we obtain the number density of grains grown at each temperature. Having calculated both the $Nv^2$ and density values for each temperature, we isolate the values of $N$ and $v$ using the time dependent nucleation rate formula, $density = (3/\pi)^{1/3} * 0.8929795 * (N/v)^{2/3}$ and using this equation in conjunction with the

Arrhenius equation described above to calculate our desired values. We choose to take the mean of all $N$ and $v$ values calculated for x values between 10 and 35 degrees Celsius to get an average approximation of the true quantities.

Once we have solved for these values, we use the Arrhenius form equations to solve for the formation energy of the crystalline bonds $\Delta E_{attachment}$ and the free energy difference at peak cluster size $\Delta G(i_c)$ using the following equations: $N \sim k1 * exp[-(\Delta E_{attachment} + \Delta G(i_c))/ k_B * T]$ and $v \sim k2 * exp[-(\Delta E_{attachment})/ k_B * T]$ where $k1$ and $k2$ are individual constants and $k_B$ and $T$ are respectively, the Boltzmann constant (eV) and temperature in Kelvin. To solve for the free energy reduction $g_{c\rightarrow a}$ and critical cluster size $i_c$, we use the following approximations: $\Delta G(i_c) \sim -g_{c\rightarrow a} * i_c + \gamma * i_c^{2/3}$ and $\Delta G(i_c) = (4 * \gamma^3)/(27 * g_{c\rightarrow a}^2)$, where $\gamma$ is the weighted surface energy of $Te$ as approximated by the Materials Project database[3]. Plugging in these values will give us both the free energy reduction from amorphous to crystalline $Te$ as well as the critical cluster size in atoms.

**Results**

Table 1 below shows the fraction area transformed as a function of time using the conversion metric of 2.87 frames per second. This table only depicts the first 10 timesteps data but was continued for each interval of frame selected. As a reminder, the intervals for 10C and 15C was 100 frames, for 20C and 25C was 50 frames, and for 30C and 35C was 20 frames. These differing timesteps were selected in correlation with the quantity of frames available for each temperature experiment. To calculate these values, the *open cv2* Python [4] library was used to mass process the frames and write the data to a CSV file for further analysis.

| 10C time (s) | 10C_afc | 15C time (s) | 15C_afc | 20C time (s) | 20C_afc | 25C time (s) | 25C_afc | 30C time (s) | 30C_afc | 35C time (s) | 35C_afc |
|---|---|---|---|---|---|---|---|---|---|---|---|
| 0.348432 | 0.000000 | 0.348432 | 0.0000 | 0.348432 | 0.0000 | 0.348432 | 0.0000 | 0.348432 | 0.0000 | 0.348432 | 0.0000 |
| 34.843206 | 0.005530 | 34.843206 | 0.0500 | 17.421603 | 0.0424 | 11.149826 | 0.0400 | 6.968641 | 0.0500 | 3.484321 | 0.0800 |
| 69.686411 | 0.016075 | 69.686411 | 0.0506 | 34.843206 | 0.1300 | 34.146341 | 0.0900 | 13.937282 | 0.1000 | 6.968641 | 0.1400 |
| 104.529617 | 0.027778 | 104.529617 | 0.1000 | 53.310105 | 0.1700 | 51.567944 | 0.1300 | 20.905923 | 0.1400 | 10.452962 | 0.1454 |
| 139.372822 | 0.023020 | 139.372822 | 0.1027 | 71.777003 | 0.2400 | 68.292683 | 0.1800 | 27.874564 | 0.1700 | 13.937282 | 0.1496 |
| 174.216028 | 0.029321 | 174.216028 | 0.1231 | 87.804878 | 0.2410 | 84.320557 | 0.2192 | 34.843206 | 0.2300 | 17.421603 | 0.1538 |
| 209.059233 | 0.042567 | 209.059233 | 0.1272 | 105.226481 | 0.2442 | 101.742160 | 0.2200 | 41.811847 | 0.3500 | 20.905923 | 0.1638 |
| 243.902439 | 0.050154 | 243.902439 | 0.1348 | 124.041812 | 0.2445 | 121.254355 | 0.2545 | 48.780488 | 0.4143 | 24.390244 | 0.1944 |
| 278.745645 | 0.052083 | 278.745645 | 0.1550 | 139.721254 | 0.2446 | 136.933798 | 0.2612 | 55.749129 | 0.4164 | 27.874564 | 0.2204 |
| 313.588850 | 0.055813 | 313.588850 | 0.1699 | 157.491289 | 0.1363 | 154.006969 | 0.2700 | 62.717770 | 0.4254 | 31.358885 | 0.3188 |

***Table 1.*** This table shows the first ten rows of data on temperature *afc* (area fraction transformed) and the timestamp recorded. Since we are only given frames, we divide frame index by 2.87, or the rate at how many frames are taken per second, to determine the time of each data point.

Given the data from our image analysis, we plotted the values and fitted them to the Arrhenius form equation for nucleation rate as expanded upon in *Item C* of the Appendix. Figure 4 below depicts the plots for each temperature trial including the data points as well as the fitted sigmoid curves to approximate the area fraction transformed over time.

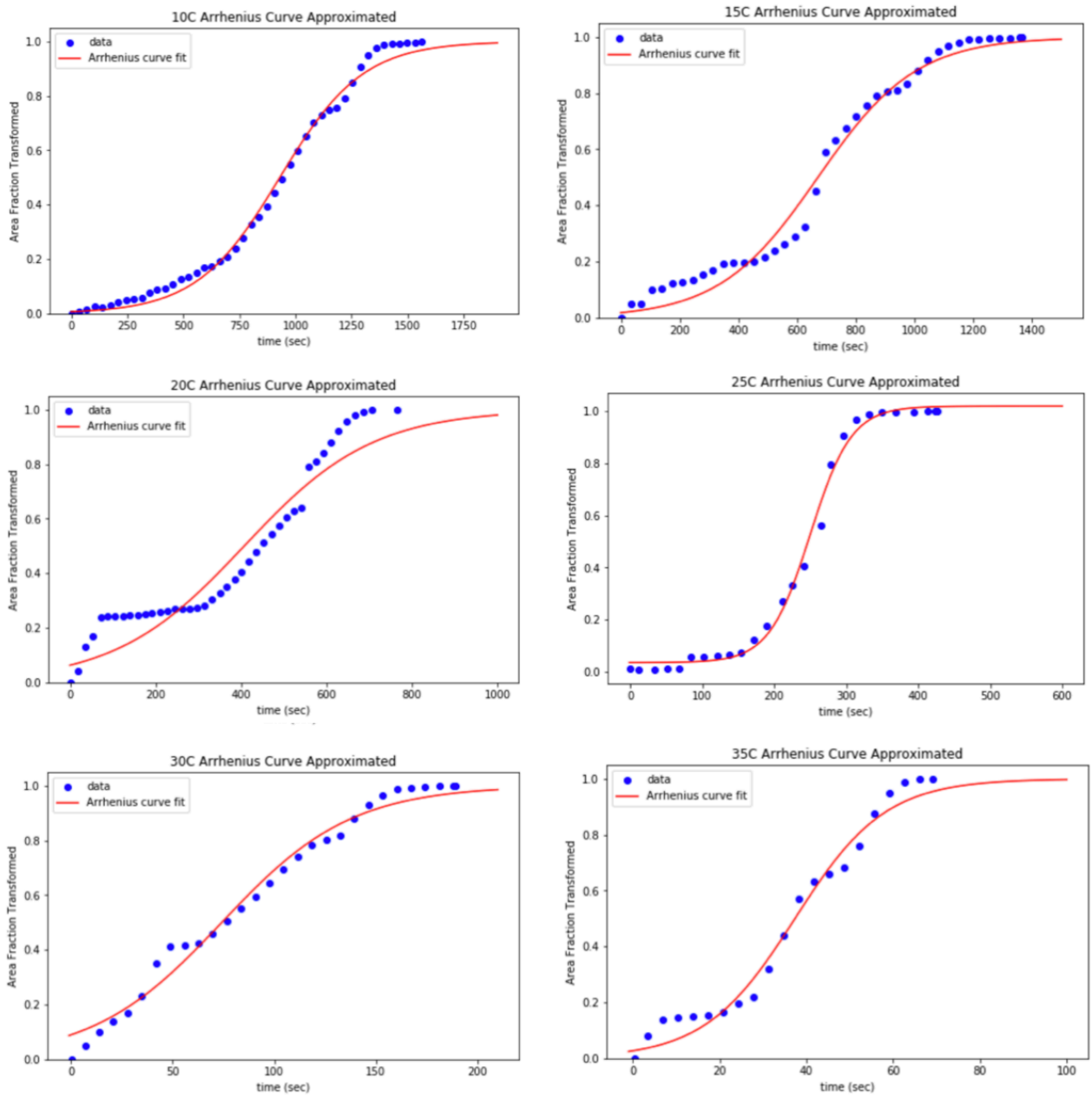


***Figure 4.*** Depicted above are the Arrhenius form fitted curves over the experimental data for area transformed over time for each of the temperature experiments.

From the above plots, we are able to determine the product $Nv^2$ as a function of temperature following the Arrhenius equation $\alpha = 1 - exp[-(\pi/3) * Nv^2 t]$. Our resulting values were averaged

across the x-range of each dataset, with the goal of obtaining a weighted mean approximation for the $Nv^2$ value. The results are depicted below in Table 2.

| Temperature (Celsius) | *Nv2* value |
|---|---|
| 10 | 1.51642973402231E-09 |
| 15 | 6.06108922502882E-09 |
| 20 | 3.52765728517786E-08 |
| 25 | 1.78528591715484E-06 |
| 30 | 9.58788943326949E-06 |
| 35 | 6.26363098285511E-05 |

***Table 2.*** Calculated $Nv^2$ values for each temperature of the experiment

With the calculated $Nv^2$ values, our next step was to estimate the number density of grains per temperature. Without micrographs, this analysis was conducted by manually counting grains per a specific region of each of the 70 $\mu$m and 140 $\mu$m frames, and then extending this numerical density to the remainder of the graph. As mentioned in the experimental procedure, the *open cv2* package was used to calculate the fraction of the region we bounded to manually count the grains. The results of our density analysis for each temperature are presented in Table 3 below.

| Temperature (Celsius) | *Density* value (grains / μm²) |
|---|---|
| 10 | 0.024505 |
| 15 | 0.027586 |
| 20 | 0.036781 |
| 25 | 0.040459 |
| 30 | 0.066206 |
| 35 | 0.073562 |

***Table 3.*** Calculated density values for each temperature of the experiment

Plugging in our values for density and $Nv^2$ into the equations $density = (3/\pi)^{1/3} * 0.8929795 * (N/v)^{2/3}$ and $\alpha = 1 - exp[-(\pi/3) * Nv^2 t]$, we isolate both $N$ and $v$. The derived values for $N$ and $v$ are given in Table 4 below.

| Temperature (Celsius) | *N* value | *v* value |
|---|---|---|
| 10 | 0.000720039906145886 | 0.00246680198996169 |
| 15 | 0.00175928921036555 | 0.00354519364699962 |
| 20 | 0.00580564734658655 | 0.0053349057290397 |
| 25 | 0.0776408562643179 | 0.0132977474748254 |
| 30 | 0.0800612922486535 | 0.0285115958377938 |
| 35 | 0.273262178485597 | 0.0596265756599407 |

***Table 4.*** Calculated average $N$ and $v$ values for each temperature of the experiment

Using our calculated values, we use the Arrhenius form equations to solve for the formation energy of the crystalline bonds $\Delta E_{attachment}$ and the free energy difference at peak cluster size $\Delta G(i_c)$ using the following equations: $N \sim k1 * exp[-(\Delta E_{attachment} + \Delta G(i_c))/ k_B * T]$ and $v \sim k2 * exp[-(\Delta E_{attachment})/ k_B * T]$ where $k1$ and $k2$ are individual constants and $k_B$ and $T$ are, respectively, the Boltzmann constant (eV) and temperature in Kelvin. Fitting the $N$ and $v$ values to the exponential forms, we derive both $\Delta E_{attachment}$ and $\Delta G(i_c)$ as shown in Figure 5 below.

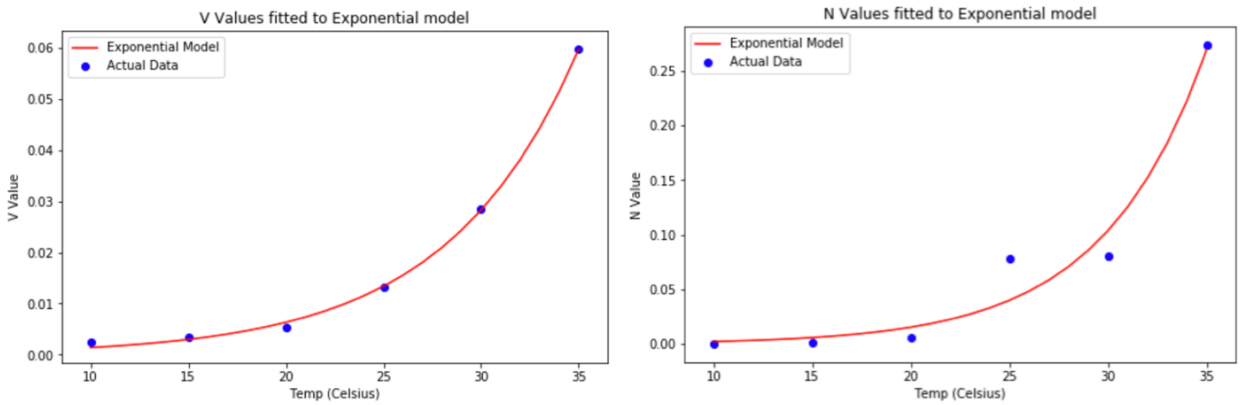


***Figure 5.*** Approximated exponential curves for $v$ and $N$ values respectively

From the above curves and the approximation equations, we find $\Delta E_{attachment}$ to be 0.0083645 eV and $\Delta G(i_c)$ to be 0.0021216 eV. To solve for the free energy reduction $g_{c\rightarrow a}$ and critical cluster size $i_c$, we use the following approximations: $\Delta G(i_c) \sim -g_{c\rightarrow a} * i_c + \gamma * i_c^{2/3}$ and $\Delta G(i_c) = (4 * \gamma^3)/(27 * g_{c\rightarrow a}^2)$, where $\gamma$ is the weighted surface energy of *Te* as approximated by the Materials Project database[3]. Plugging in these values, we find $g_{c\rightarrow a}$ to be 0.0083564 eV and critical cluster size $i_c$ to be 1.2908 *Te* atoms. See *Item D* in the Appendix of this report for a detailed review of the derivation to find $g_{c\rightarrow a}$ and $i_c$. The following section discusses these results in detail, providing context to the values and exploring the confidence and uncertainty of specific values – exploring the potential error bounds with the derived values and discussing any factors that potentially influenced these results.

**Discussion**

The primary assumption made while assessing the nucleation rate of *Te* onto a substrate is that the thin film growth can be modelled as a two-dimensional quantity. This fact paired with the inconsistent lighting and image quality across temperature ranges, introduced a variable of uncertainty into our analysis. Beginning with the calculation of the area fraction transformed over time, the image classification algorithm used depended on *open cv2* to accurately find and classify clusters, ultimately providing a reasonable estimate on the true transformation rate. For instance, the unaltered classification provided data that resulted in poor results shown below in Figure 6.

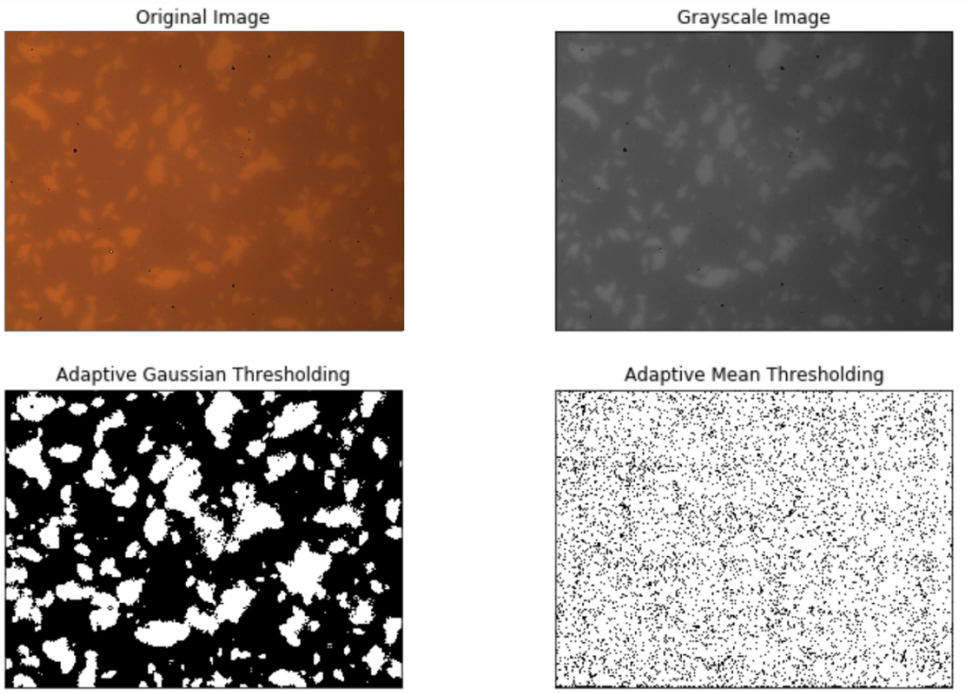


***Figure 6.*** Images processed using Python *open cv2* library [4]. Bottom two images are produces using the grayscale image and applying thresholding techniques to classify nucleation.

As seen from the above images, the adaptive gaussian thresholding technique provided the most accurate black and white frame for image classification. In this experiment, our image data have different lighting conditions in different areas and a simple threshold will not be able to

binarize the pixels for classification. The algorithm used determines the threshold for a pixel based on a small region around it and provides different thresholds for different regions of the same image which gives better results for images with varying illumination [5].

With this classification method, our calculations for area transformed as a function of time became more accurate. Due to the large volume of frames for each temperature, images were selected at intervals to not overload the computing system. As mentioned in the Results section, the data was fitted to the Arrhenius form equation for area transformed, $\alpha = 1 - exp[-(\pi/3) * Nv^2 t]$, and the resulting curves appear to follow a sigmoid shape, which is to be expected given classical nucleation theory[2]. These curves are displayed below.

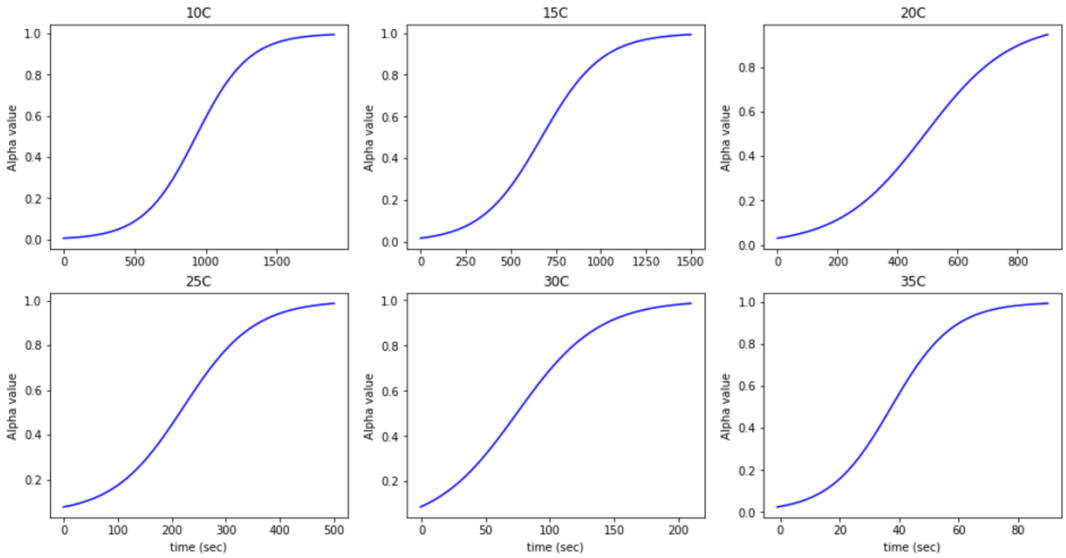


***Figure 7.*** Approximated curves for area fraction transformed over time (seconds)

Upon calculating the values for $Nv^2$, it is evident that the weighted mean is a fair estimate of the quantity but given our less than 100% accurate image classification algorithm, there still remains a large uncertainty regarding the true value. Knowing the qualitative factors that might have influenced our true derivation of $Nv^2$, we estimate the uncertainty using a 95% confidence interval since we have an array of values for $Nv^2$ spanning the number of data points. From the

data mean, size, and standard deviation, we calculate the following uncertainty for each temperature in the table below. The functions and programs written to measure uncertainty are explained in greater detail in *Item B* of the Appendix.

| Temperature (Celsius) | 95% confidence interval for $Nv^2$ value |
|---|---|
| 10C | (6.47e-10 to 2.39e-9) |
| 15C | (1.29e-9 to 1.08e-8) |
| 20C | (-2.23e-10 to 7.08e-8) |
| 25C | (-4.55e-7 to 0.00000403) |
| 30C | (-0.00000111 to 0.0000203) |
| 35C | (-0.00000696 to 0.000132) |

***Table 5.*** Calculated 95% confidence interval for $Nv^2$ values

For the density estimates, there isn't as quantitative a way to measure the uncertainty but knowing that the counting of grains in each region was manual, there is a high possibility of human error. Additionally, we assumed that the density of one small region extends to the rest of the thin film frame. This assumption could also have led to skewed estimates. In calculating $N$ and $v$, we apply a similar 95% confidence interval. The results of this analysis are presented below.

| Temperature (Celsius) | 95% confidence interval for $N$ | 95% confidence interval for $v$ |
|---|---|---|
| 10C | (-0.000103 to 0.000801) | (0.000898 to 0.00127) |
| 15C | (-0.000343 to 0.0019) | (0.00107 to 0.00167) |
| 20C | (-0.000516 to 0.00238) | (0.00143 to 0.00258) |
| 25C | (-0.0242 to 0.058) | (0.00246 to 0.00712) |
| 30C | (-0.0124 to 0.049) | (0.007 to 0.0148) |
| 35C | (-0.228 to 0.774) | (0.0134 to 0.0315) |

***Table 6.*** Calculated 95% confidence intervals for $N$ and $v$ for each temperature

As we can see from these values above, there exists an elaborate range between which the true $N$ and $v$ values can exist. This uncertainty is only increased with our prior uncertainty in image classification and as a result adds more variability to our data. We conduct a similar analysis for our calculated $\Delta E_{attachment}$ and $\Delta G(i_c)$ values which we found to be 0.0083645 eV and 0.0021216 eV respectively. The 95% confidence interval for $\Delta E_{attachment}$ is (0.00794 to 0.00878) and the 95% confidence interval for $\Delta G(i_c)$ is (0.00176 to 0.00248). While these intervals may seem small, it is important to note that this uncertainty is expounded by the variability from the prior analysis and if we were to upper bound all of our estimates in this analysis, the resulting values for $\Delta E_{attachment}$ and $\Delta G(i_c)$ would be drastically different. Additionally, $\Delta E_{attachment}$ is the energy barrier associated with the breaking of the amorphous bonds, and the formation of the crystalline bonds and for our calculations it makes sense that the formation energy barrier would be greater than $\Delta G(i_c)$, the free energy of the system.

We extend our uncertainty analysis to derived values for $g_{c\rightarrow a}$ = 0.0083564 eV and the critical cluster size $i_c$ of 1.2908 $Te$ atoms more qualitatively. Seeing our expansive range of uncertainty in the values leading up to the derivation of the thermal energy barrier to nucleation and the critical nucleus size, it is a reasonable assumption that the calculated values only provide a frame of reference in order of magnitude to what the true quantities are. Furthermore, improving the accuracy of our image classification algorithm, collecting more data points, and finding alternate methods of calculating grain density would drastically improve the accuracy of our results and increase the certainty of our values.

## Conclusion

Upon analyzing the image data of the *Te* thin films, we were able to derive approximations for the nucleation rate, $N$, the growth velocity of the grain, $v$, and calculate the formation energy of the crystalline bonds $\Delta E_{attachment}$ and the free energy difference at peak cluster size $\Delta G(i_c)$, ultimately allowing us to estimate the free the free energy change per unit volume $g_{c\rightarrow a}$ – during the amorphous to crystalline transition – and estimate the critical nucleus size $i_c$ in atoms governing the growth kinetics. While the process introduced extraneous error, such as the manual calculation of density and the algorithm-approximated area fraction transformed data, this study developed a reasonable bound on the key quantities governing *Te* thin film growth on substrates. We found that the formation energy of the crystalline bonds is greater than the free energy difference of peak cluster size which follows our intuition and agrees with classical nucleation theory. Furthermore, while the estimated critical nucleus size was around 1.3 atoms, our uncertainty analysis revealed that this was fairly consistent with the upper bound and close to the true value by one order of magnitude. Further analysis in tuning the image classification method and approximating the grain density of thin films at various temperatures will enhance the accuracy of our results and provide closer estimates of the free the free energy change per unit volume $g_{c\rightarrow a}$ and critical nucleus size $i_c$ in atoms governing the growth kinetics. The implications of this research will allow innovators to enhance applications in sensor technologies and flexible displays, seeing as *Te* thin films can be effectively controlled and grown on substrates at low temperatures for industrial processing.

**Acknowledgements**

We are grateful to the Javey Research Group for their experimental data, providing us with the images and videos of *Te* thin film growth at various temperatures. We would also like to acknowledge Professor Daryl Chrzan for his white paper and background context on this topic. Additionally, we acknowledge the MSE 130 course staff for their help and guidance throughout this laboratory experiment.

**References**


1. C. Zhao, H. Batiz Guerrero, B. Yasar, H. Kim, W. Ji, M. C. Scott, D. C. Chrzan, and A. Javey, "One-dimensional tellurium single-crystal arrays by low-temperature evaporation and crystallization," (2020), submitted.
2. R. Becker and W. Döring, Annalen der Physik 416, 719 (1935).
3. http://materialsproject.org/
4. Jupyter Notebook and *open cv2* among other Python libraries
5. https://docs.opencv.org/3.4/d7/d4d/tutorial_py_thresholding.html

# Appendices

## *Item A:*

**Image Classification Notebook**

*Conducted for frame data in experiments at 20 degrees Celsius*

```
string = '30C00203.png'
```

```
img = cv2.imread(string,0)
img = cv2.medianBlur(img,5)

thresh, vals = cv2.threshold(img, 127, 255, cv2.THRESH_BINARY)

bw = cv2.adaptiveThreshold(img,255,cv2.ADAPTIVE_THRESH_GAUSSIAN_C,\
            cv2.THRESH_BINARY,999,0)

titles = ['Grayscale Image','Adaptive Gaussian Thresholding']
images = [img, bw]

plt.figure(figsize = (10,8))
for i in range(2):
    plt.subplot(2,2,i+1),plt.imshow(images[i],'gray')
    plt.title(titles[i])
    plt.xticks([]),plt.yticks([])
plt.show()
```

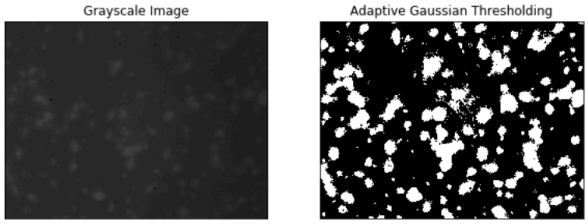


```
a = np.count_nonzero(bw)
b = len(bw)*len(bw[0])

area_frac_transformed = a/b
area = str(area_frac_transformed)[:6]
area
```

```
'0.2149'
```

## *Item B:*

```
nv2 = {}
for i in range(len(temps)):
    nv2[temps[i]] = nv2_vals[i]
nv2
```

```
{'10C': 1.5164297340223137e-09,
 '15C': 6.06108922502882e-09,
 '20C': 3.5276572851778596e-08,
 '25C': 1.7852859171548411e-06,
 '30C': 9.587889433269485e-06,
 '35C': 6.263630982855114e-05}
```

**Uncertainty Analysis of calculated $Nv^2$ values** ¶

Since we took the mean nv2, you can use $r^2$ value or confidence interval to determine how sure this $Nv^2$ value is. Also, since the Arrhenius curve model was fitted over data with a relatively poor accuracy in determining overall grain growth, the basis model is not 100% accurate in depicting area transformed, which is an factor to take into account when judging the validity of our $Nv^2$ values.

```
def uncertainty_NV2(df):
    nv2 = []
    for i in range(len(df[0])):
        t = np.log(1 - df[1][i]) * (-3/math.pi) * (1/(df[0][i]**3))
        nv2.append(t)
    nv2 = nv2[2:]
    mean = np.mean(nv2)
    length = len(nv2)
    std = statistics.stdev(nv2)
    return (mean, length, std)
```

```
uncertainty_NV2(d35)
```

```
(6.263630982855114e-05, 48, 0.000246098559245255)
```

*Item C:*

**Generating Arrhenius Curves from Data**

```
df = pd.read_csv("10C_cleaned.csv")

data_x = df['time (s)'].tolist()
data_y = df['normalized'].tolist()

def fsigmoid(x, a, b):
    return 1.0 / (1.0 + np.exp(-a*(x-b)))

xdata = data_x
ydata = data_y

popt, pcov = curve_fit(fsigmoid, xdata, ydata, method='dogbox', bounds=([0, 600],[0.01, 1200]))

x = np.linspace(-1, 1900, 50)
y = fsigmoid(x, *popt)
d10 = [x,y]

pylab.figure(figsize=(8,5))
pylab.plot(xdata, ydata, 'bo', label='data')
pylab.plot(x,y, 'r', label='Arrhenius curve fit')

pylab.title('10C Arrhenius Curve Approximated');
pylab.xlabel('time (sec)');
pylab.ylabel('Area Fraction Transformed');

pylab.ylim(0, 1.05)
pylab.legend(loc='best')
pylab.show()
```

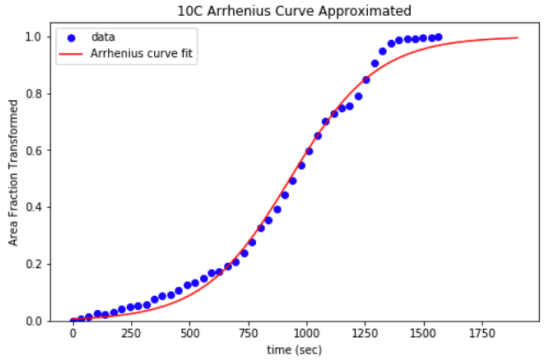


*Item D:*

### Step VII: Estimating $i_{critical}$ and $g_{c\to a}$

*Calculating critical nucleus size and the free energy difference between amorphous and crystalline phases*

We know ΔG(j) = -$g_{c\to a}$ * $j + \gamma j^{2/3}$ ***and*** $\Delta G(i_c) = (4\gamma^3)/(27 * (g_{c\to a})^2)$. Combining the two equations by substituting γ in terms of $g_{c\to a}$ and $\Delta G(i_c)$ we get the following equality: $\Delta G(ic) = -gca * i_c + i_c^{2/3} * [(\Delta G(ic) * 27*gca^{2})/4]^{1/3}$. From the Materials project, https://materialsproject.org/materials/mp-19/, the surface energy, gamma (γ) for *Te* is given as 0.01 eV/Å$^2$

In [38]:
```
gamma = 0.01 # from materialsproject database
```

In [39]:
```
gca = ((4*gamma**3)/(27*dG))**(1/2)
gca
```

Out[39]:
```
0.008356423479455522
```

Knowing our $g_{c\to a}$ value as **gca = 0.008356423479455522 eV** and gamma as **γ = 0.01 eV/Å$^2$** we can now plug these measured quantities into the following equation: $\Delta G(i_c) = -g_{c\to a} * i_c + \gamma * i_c^{2/3}$

In [40]:
```
c = -1*gca + gamma
i_critical = dG/c
i_critical
```

Out[40]:
```
1.2908192023002676
```

Given the energy barrier to nucleation, our estimated size of the critical nucleus is $i_{critical}$ **= 1.2908192023002676 atoms**, and the free energy difference between the amorphous and crystalline phases is $g_{c\to a}$ **= 0.008356423479455522 eV**. Reflecting on these estimates, we look at the confidence level of our values and perform **uncertainty analysis** to understand how accurate our estimates are and what factors may have skewed our results.